

Accessing acyclic vicinal tetrasubstituted stereocenters via biomimetic Cu/squaramide cooperative catalysed asymmetric Mannich reactions

Received: 8 December 2024

Accepted: 3 September 2025

Published online: 07 October 2025



Wen-Run Zhu^{1,2,4}, Ze-Long Ouyang^{1,4}, Xuzhao Du^{3,4}, Yun-Zhe Li^{1,4},
Xiao-Yi Deng¹, Yu-Jie Xue², Jian-Xin Zhou², Peiyuan Yu³✉, Gui Lu¹✉,
Albert S. C. Chan¹ & Jiang Weng¹✉

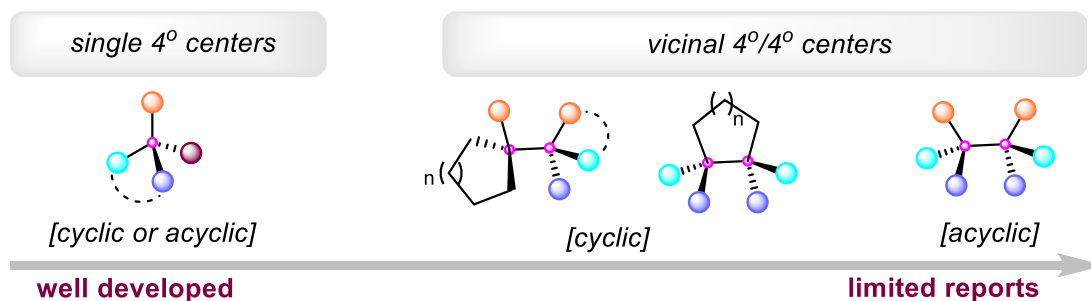
The catalytic asymmetric Mannich reaction offers efficient approaches for the simultaneous construction of a C–C bond and two adjacent stereocenters in a single step. However, employing the Mannich reaction to create two neighboring, fully substituted carbon stereocenters in acyclic systems presents significant challenges and remains largely unexplored. Inspired by class II aldolases found in nature, we report here a biomimetic copper/squaramide cooperative catalysis strategy for asymmetric Mannich reactions between challenging acyclic ketimines and α -substituted β -keto esters. The highly functionalized Mannich adducts featuring vicinal and acyclic tetrasubstituted stereocenters are obtained, and exhibit good yields and excellent stereoselectivities (up to >19:1 dr and 99% ee). The versatile utility of these enantioenriched products is further highlighted by their diverse transformations with complete diastereocontrol. Mechanistic studies and DFT calculations support the novel cooperative roles of copper and squaramide in substrate activation and stereoselectivity control.

C(sp³)–C(sp³) bonds constitute the framework of numerous bioactive natural products, pharmaceuticals, and functional materials. It has been suggested that a higher prevalence of sp³-hybridized chiral carbons is strongly associated with improved potency, selectivity, and patentability in drug discovery^{1–4}. The development of efficient methods that can simultaneously form C(sp³)–C(sp³) bonds and control stereochemistry is thus of long-standing interest in synthetic chemistry^{5–9}. However, achieving diastereo- and enantioselective construction of vicinal, fully substituted carbon stereocenters remains a formidable challenge, primarily due to the unfavorable

thermodynamic and kinetic effects resulting from increased steric hindrance^{10,11}. Despite various efficient strategies being elaborated to achieve this goal, the majority of these methods result in the formation of at least one quaternary stereocenter within a cyclic system^{12,13}. In contrast, the stereoselective construction of C(sp³)–C(sp³) bonds bearing two neighboring quaternary stereocenters within an acyclic skeleton presents a particularly challenging task, owing to the increased rotational freedom and the severe steric congestion during C(sp³)–C(sp³) bond formation^{14–16}, and remains largely underdeveloped (Fig. 1A)^{17–23}.

¹State Key Laboratory of Anti-Infective Drug Discovery and Development, Guangdong Provincial Key Laboratory of Chiral Molecule and Drug Discovery, School of Pharmaceutical Sciences, Sun Yat-sen University, Guangzhou, P. R. China. ²School of Pharmacy, Guangdong Pharmaceutical University, Guangzhou, P. R. China. ³Department of Chemistry and Guangming Advanced Research Institute, Southern University of Science and Technology, Shenzhen, P. R. China. ⁴These authors contributed equally: Wen-Run Zhu, Ze-Long Ouyang, Xuzhao Du, Yun-Zhe Li. ✉e-mail: yupy@sustech.edu.cn; lugu@mail.sysu.edu.cn; wengj2@mail.sysu.edu.cn

A) Increasing challenges in the construction of fully substituted stereocenters



B) Catalytic asymmetric Mannich reactions: varieties of stereocenters generated

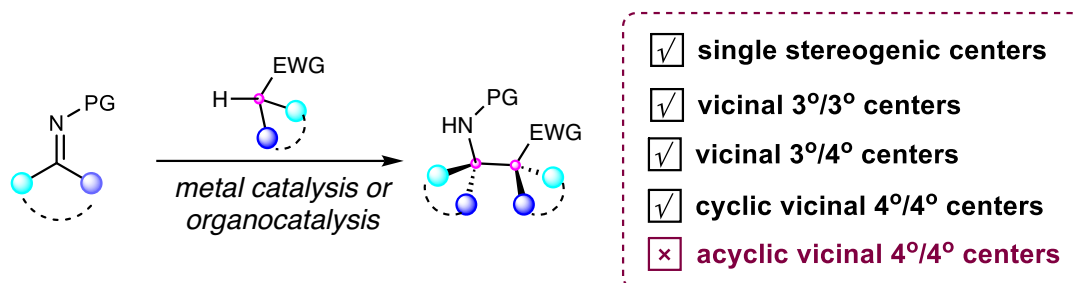
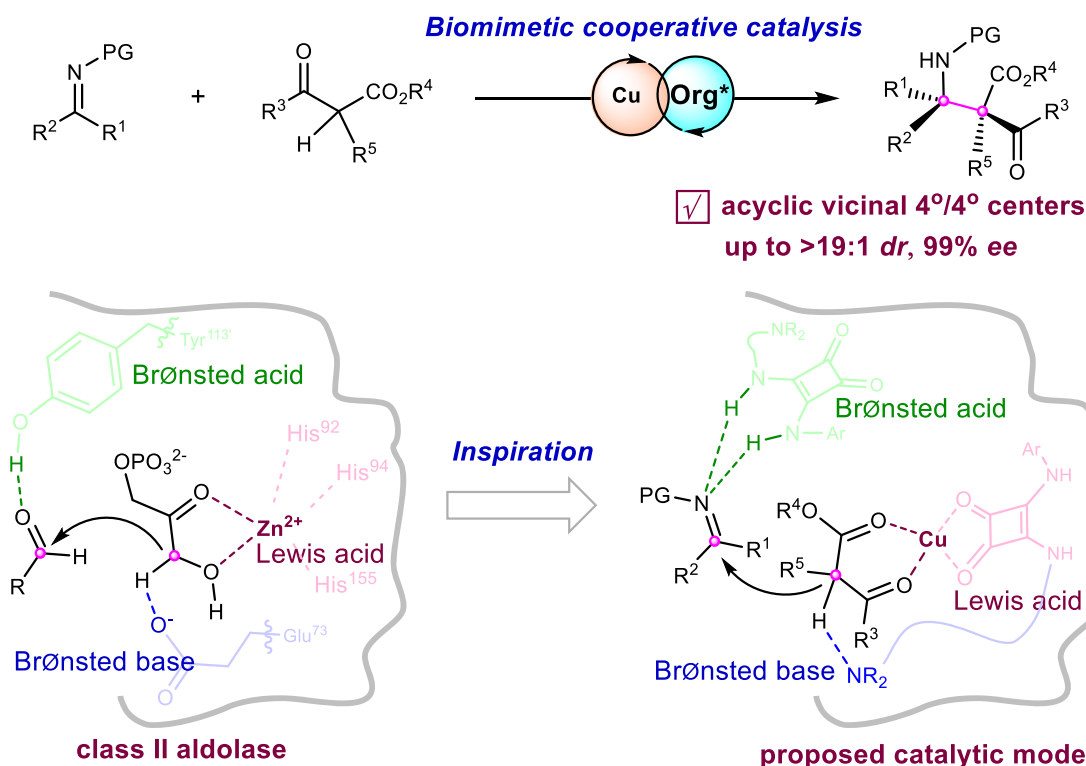
C) **This work:** Stereoselective generation of acyclic vicinal full-substituted stereocenters via biomimetic asymmetric Mannich reactions

Fig. 1 | Construction of fully substituted stereocenters and development of biomimetic asymmetric Mannich reactions leading to the generation of acyclic vicinal 4°/4° stereocenters. A Increasing challenges in the construction of fully

substituted stereocenters. **B** Catalytic asymmetric Mannich reactions: varieties of stereocenters generated. **C** Stereoselective generation of acyclic vicinal full-substituted stereocenters via biomimetic asymmetric Mannich reactions.

The Mannich reaction is one of the most classical C(sp³)-C(sp³) bond formation reactions in organic synthesis^{24–29}. Catalytic asymmetric Mannich reactions represent an attractive approach for producing a diverse array of optically enriched amines and derivatives. Since the pioneering demonstrations of catalytic enantioselective Mannich reactions in the late 1990s, significant advancements have been made by leveraging chiral organometallic catalysts³⁰ and organocatalysts^{31–34}, facilitating the stereocontrolled formation of single or two adjacent stereocenters. To date, constructing vicinal tertiary/tertiary^{35–39} and tertiary/quaternary^{35,40–44} stereocenters have been well established through diastereo- and enantioselective Mannich reactions (Fig. 1B). Nonetheless, the exploration of asymmetric Mannich reactions for the synthesis of vicinal full-substituted stereocenters remains relatively unexplored^{45–54}. Notably, these limited examples have consistently employed cyclic imines and/or cyclic nucleophilic donors, leading to the formation of at least one quaternary stereocenter embedded within a cyclic structure^{45–51}. To the best of our knowledge, there have been no reports on the asymmetric Mannich reaction for the construction of vicinal acyclic tetrasubstituted stereocenters.

Biomimetic asymmetric catalysis that emulates enzyme function has long been a primary goal in synthetic chemistry^{52,53}. In nature, aldolases have evolved as highly effective enzymes that catalyze asymmetric aldol reactions, providing a robust strategy for the stereoselective assembly of carbon-carbon bonds. Among the two known classes of aldolases, class II aldolases utilize a metal ion cofactor (typically Zn²⁺), which acts as a Lewis acid, to activate the aldol donor via coordination to the generated enolate⁵⁴. Concurrently, Brønsted basic residues within the enzyme facilitate the deprotonation and enolate formation, while Brønsted acidic residues activate the electrophilic aldehyde (Fig. 1C). However, biomimetic asymmetric catalysis inspired by class II aldolases has been relatively overlooked, especially when compared to the extensively studied enamine catalysis based on class I aldolases. Inspired by the cooperative action of metallic Lewis acids, Brønsted bases, and Brønsted acids in class II aldolases, we present a copper/squaramide cooperative catalysis system designed for asymmetric Mannich reactions. By mimicking the features of class II aldolases, we propose that copper salts, acting as Lewis acids, can effectively activate acyclic β-keto esters. Simultaneously, tertiary amine-squaramide bifunctional organocatalysts can engage in multiple hydrogen-bonding interactions with the substrates, thereby facilitating challenging asymmetric Mannich reactions involving acyclic ketimines and acyclic trisubstituted carbon nucleophiles. Furthermore, this biomimetic cooperative catalysis system features a more suitable chiral pocket than that of a single chiral metal- or organocatalyst, enabling the formation of vicinal acyclic tetrasubstituted stereocenters in a crowded environment with precise control over both diastereo- and enantioselectivity.

Results

Reaction optimization. To evaluate our hypothesis, we selected β,γ-alkynyl-α-imino ester **1a** and ethyl 2-methylacetoacetate **2a** as model substrates for the investigation of the asymmetric Mannich reaction (Table 1). Inspired by the successful use of bifunctional organocatalysts in asymmetric Mannich-type reactions, we first screened several chiral bifunctional thiourea⁵⁵ and squaramide^{56,57} organocatalysts. We hypothesized that these bifunctional organocatalysts, which incorporate a Brønsted-basic tertiary amine alongside hydrogen-bond donors, could simultaneously activate both ketimine **1a** and dicarbonyl compound **2a** through cooperative hydrogen-bonding interactions. Initial screening with squaramide catalysts alone (Table 1, entries 1–3, and see also the Supplementary Information) afforded the desired amino acid derivative **3a** with adjacent non-cyclic tetrasubstituted stereocenters. However, despite high diastereoselectivity, yields remained low to moderate (32–50%) with poor enantioselectivity (<10% ee). Prior

studies suggested Lewis-acidic copper salts could activate dicarbonyl compounds^{58–61}. Thus, the combined catalysis of squaramides and copper salts were examined, and we were pleased to find that improved yields and enantioselectivities were obtained when copper(I) thiophene-2-carboxylate (CuTC) was added as the co-catalyst (Table 1, entries 4–6). Among them, the cinchona alkaloid-derived squaramide **Cat-3** performed best. Consequently, we screened other cinchona alkaloid-based catalysts (e.g., sulfonamides, thioureas; entries 7–10), but **Cat-3** retained superior stereoselectivity (entry 6). Further screening of other squaramide catalysts (Table S1 and Supplementary Information) did not enhance stereoselectivity. Noteworthy, the diastereomer **Cat-16** of **Cat-3** produces the opposite enantiomer of the Mannich reaction product **3a** in 52% yield, 60:40 dr, and 35% ee (entry 16, Table S1 and Supplementary Information). Evaluation of alternative copper salts (CuI, Cu₂O, and Cu(MeCN)₄PF₆) confirmed CuTC as optimal. Notably, CuI slightly improved diastereoselectivity at the expense of enantioselectivity (entry 11). Solvent screening (THF, toluene, DCE, MeCN, acetone, chlorobenzene, 1,4-dioxane; entries 14–20) identified DCM as optimal (entry 6). Lowering the reaction temperature increased ee from 87% to 90%, albeit with moderate diastereoselectivity (entry 21). The addition of additives (molecular sieves, Na₂SO₄, MgSO₄) enhanced diastereoselectivities but significantly reduced yields (entry 22, and Table S3 of Supplementary Information). Chiral bisoxazoline ligands^{62–64} for copper improved diastereoselectivity marginally without increasing ee (entries 23–26). Increasing **Cat-3** loading to 20 mol% afforded **3a** in 72% yield, 80:20 dr, and 93% ee (entry 27). To further improve diastereoselectivity, we optimized CuTC/CuI and **Cat-3** loadings using MgSO₄ as an additive (entries 28–31). Ultimately, the reaction with 10 mol% CuTC and 25 mol% **Cat-3** in DCM (2 mL) at 0 °C delivered optimal stereoselectivities of 94% ee and 90:10 dr (entry 30).

Scope of acyclic α-substituted β-keto esters. With optimized reaction conditions in hand, we explored the scope of the transformation using a series of acyclic β-keto esters in the presence of CuTC and **Cat-3**. As illustrated in Fig. 2, acyclic α-alkylated β-keto esters with various substituents at R¹ reacted efficiently with ketimines **1a** (Ar = Ph) and **1m** (Ar = 2-thiophene). Regardless of whether the steric bulk at R¹ was decreased or increased, the corresponding **3a–3d**, **3h–3m** featuring two contiguous and acyclic chiral stereocenters were isolated in moderate to good yields (47–78%), along with high diastereoselectivities (dr ranging from 78:22 to >95:5), and excellent enantioselectivities (85–99% ee). Furthermore, substrates containing either a methyl ester (**3e** and **3g**) or a benzyl ester (**3f**) were also compatible with the reaction; however, using more sterically hindered β-keto benzyl ester resulted in a decreased yield and ee value (**3f**). In addition, the conversion of β-keto esters with α-chloro substituents to the desired product **3n** was feasible, although the stereoselectivity was poorly controlled. The β-keto esters bearing an α-ethyl group were also smoothly converted to the desired product **3o** in high yield with 82:18 dr and 98% ee. Finally, we also evaluated ethyl 2-methylacetoacetate with representative ketimines, affording the corresponding products **3p** and **3q** in moderate yields with high levels of stereocontrol.

Scope of the β,γ-alkynyl-α-imino esters. Next, the substrate scope of β,γ-alkynyl-α-imino ester was then investigated, as shown in Fig. 3. Various 1-alkynyl N-Boc ketimino esters bearing electron-donating (such as Me, MeO, ^tBu, and acetylene) or electron-donating groups (such as CF₃, F, Cl, and Br) at the ortho, meta or para positions of the phenyl group were all compatible to the reaction conditions. This led to the formation of highly functionalized products **4a–4q** in high yields (up to 82%), accompanied by excellent enantioselectivities (90–99% ee) and diastereoselectivities (generally >95:5 dr). Furthermore, when the aryl moiety was bulky 1-naphthyl, 2-naphthyl group or heterocycle, the desired products (**4r–4t**) were also afforded in high yields with excellent enantioselectivities (94–99% ee) and diastereoselectivities (>95:5 dr). Notably, when the aryl ring was replaced with a

Table 1 | Optimization of reaction conditions^a

Entry	Copper salt (x mol%)	Catalyst (y mol%)	Solvent	Ligand	Yield (%) ^b	<i>Dr</i> ^c	ee (%) ^c
1	–	Cat-1 (10)	DCM	–	32	95:5	2
2	–	Cat-2 (10)	DCM	–	49	90:10	7
3	–	Cat-3 (10)	DCM	–	50	95:5	3
4	CuTC (10)	Cat-1 (10)	DCM	–	53	84:16	4
5	CuTC (10)	Cat-2 (10)	DCM	–	60	69:31	64
6	CuTC (10)	Cat-3 (10)	DCM	–	70	66:34	87
7	CuTC (10)	Cat-4 (10)	DCM	–	64	90:10	<5
8	CuTC (10)	Cat-5 (10)	DCM	–	31	80:20	<5
9	CuTC (10)	Cat-6 (10)	DCM	–	67	67:33	71
10	CuTC (10)	Cat-7 (10)	DCM	–	50	95:5	<5
11	CuI (10)	Cat-3 (10)	DCM	–	54	86:14	71
12	Cu ₂ O (10)	Cat-3 (10)	DCM	–	36	95:5	54
13	Cu(MeCN) ₄ PF ₆ (10)	Cat-3 (10)	DCM	–	52	70:30	16
14	CuTC (10)	Cat-3 (10)	THF	–	67	66:34	85
15	CuTC (10)	Cat-3 (10)	Toluene	–	45	87:13	23
16	CuTC (10)	Cat-3 (10)	DCE	–	40	75:25	22
17	CuTC (10)	Cat-3 (10)	CH ₃ CN	–	70	60:40	79
18	CuTC (10)	Cat-3 (10)	acetone	–	64	67:33	85
19	CuTC (10)	Cat-3 (10)	PhCl	–	45	66:34	75
20	CuTC (10)	Cat-3 (10)	1,4-dioxane	–	71	66:34	83
21 ^d	CuTC (10)	Cat-3 (10)	DCM	–	70	60:40	90
22 ^{d,e}	CuTC (10)	Cat-3 (10)	DCM	–	40	70:30	92

Table 1 (continued) | Optimization of reaction conditions^a

Entry	Copper salt (x mol%)	Catalyst (y mol%)	Solvent	Ligand	Yield (%) ^b	<i>Dr</i> ^c	ee (%) ^c
23 ^d	CuTC (10)	–	DCM	L1	29	80:20	15
24 ^d	CuTC (10)	Cat-3 (10)	DCM	L1	40	60:40	42
25 ^d	CuTC (10)	Cat-3 (10)	DCM	L2	43	75:25	4
26 ^d	CuTC (10)	Cat-3 (10)	DCM	L3	56	75:25	17
27 ^d	CuTC (10)	Cat-3 (20)	DCM	–	72	80:20	93
28 ^{d,e}	CuI (15)	Cat-3 (30)	DCM	–	62	78:22	79
29 ^{d,e}	CuTC (15)	Cat-3 (30)	DCM	–	72	70:30	90
30 ^{d,e}	CuTC (10)	Cat-3 (25)	DCM	–	71	90:10	94
31 ^{d,e}	CuTC (10)	Cat-3 (30)	DCM	–	70	92:8	85

[illegible]

²¹Isolated yield of **3a**.

Determined by chiral-phase HPLC analysis.

^dReaction conducted at 0 °C.

MgSO₄ (1.0 eq) was used. **Cat-1-Cat-7** = bifunctional organocatalysts. **L-1**–**L-3** = chiral bisoxazoline ligands.

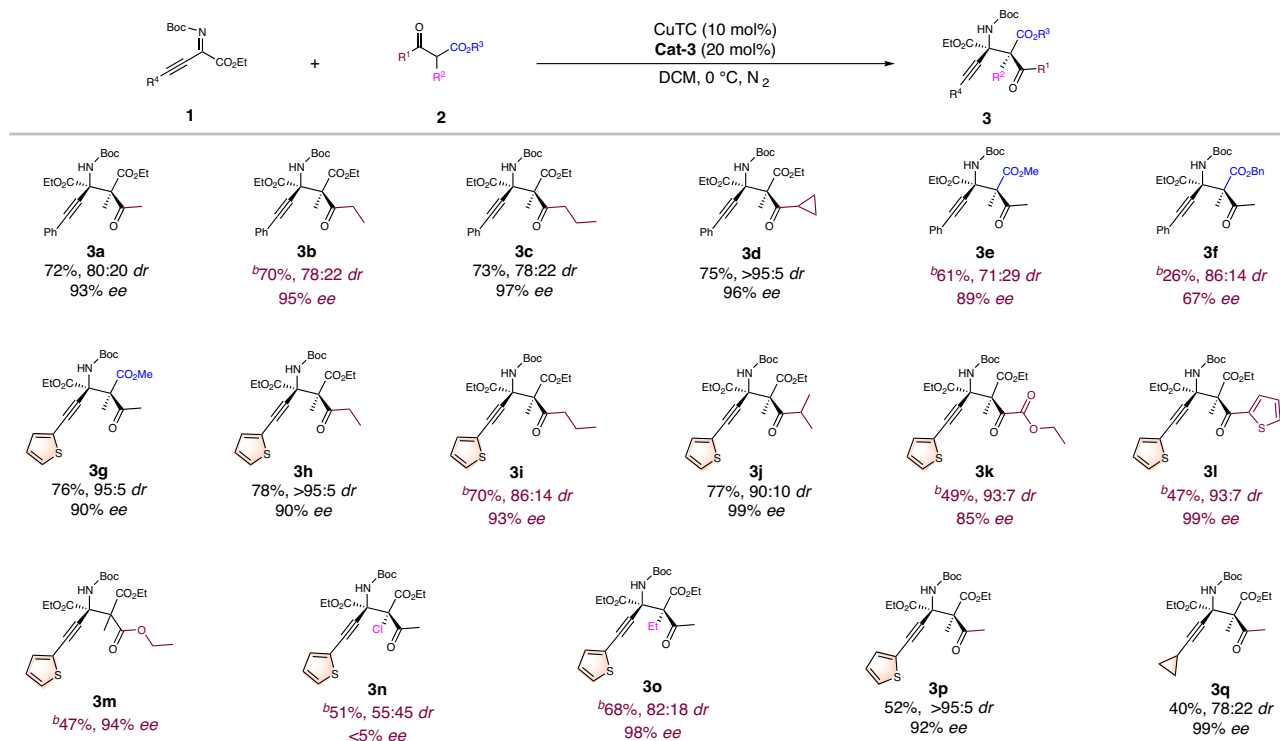


Fig. 2 | Scope of acyclic α -substituted β -keto esters. Conditions: **1** (0.10 mmol), **2** (0.12 mmol), CuTC (10 mol%), Cat-3 (20 mol%), DCM (2.0 mL), at 0 °C for 30–48 h. ^b Conditions: **1** (0.10 mmol), **2** (0.12 mmol), CuTC (10 mol%), Cat-3 (25 mol%), MgSO₄ (1.0 eq), DCM (2.0 mL), at 0 °C for 30–48 h. Boc tert-butoxycarbonyl.

trimethylsilyl group, the resulting trimethylsilyl-derived product **4u**, which can be easily transformed following deprotection, was obtained with an 80% yield, 99% ee, and >95:5 dr. Additionally, when the substrates were switched to the N-Cbz protected ketimino ester (**4w**) or the methyl ester (**4v**), the corresponding products were still obtained with good yields and excellent ee values. Unfortunately, no product formation was observed when the alkyne moiety of imino esters is replaced with alkyl, alkenyl, or aryl groups (for unsuccessful substrates, see Supplementary Information), which we attribute to reduced electrophilicity and increased steric hindrance.

Scale-up synthesis and synthetic applications. Considering the significance of highly functionalized amino acid derivatives that contain two vicinal acyclic stereocenters, we investigated the practicality of the present methodology (Fig. 4). First, we scale-up the reaction using 2.0 mmol of the starting material under standard reaction conditions. The corresponding product **3d** was afforded with comparable results (75% yield, >95:5 dr, 94% ee). Furthermore, the product **3d** could be smoothly converted to the alkyl-substituted compound **5** via hydrogenation using Pd/C, giving 96% yield and with 91% ee. Moreover, we successfully achieved the selective reduction of the ketone moiety using NaBH₄. Notably, under the reductive reaction conditions, the resulting hydroxyl group participated in an intramolecular ester exchange reaction, ultimately leading to the formation of the five-membered lactone **6**, which bears three contiguous chiral centers. The N-Boc protecting group of **6** was readily removed by treatment with trifluoroacetic acid, without disrupting the lactone ring and compromising the optical purity. Moreover, the ethynyl group in product **4h** facilitated its application in CuAAC click reactions, as exemplified by the facile synthesis of enantioenriched **8** in 97% yield and with >95:5 dr and 96% ee. The absolute configuration of **9** was definitively determined as (2S, 3R, 4R) by X-ray diffraction (CCDC 2339871 (**9**) and CCDC 2452561 (**1p**) contain the supplementary crystallographic data for this paper. This data can be obtained free of charge from The Cambridge Crystallographic Data Centre).

Control experiments and mechanistic studies. To gain insight into the mechanism of this copper/squaramide cooperatively catalyzed asymmetric Mannich reaction, a series of mechanistic investigations were conducted. First, when the ester groups in substrates **1** or **2** were replaced with other electron-withdrawing groups such as -CF₃ or -CN, no expected Mannich products were detected (Fig. 5a, b). These results indicate that the ester groups in substrates **1** and **2** play an essential role in facilitating interactions with the catalyst. Furthermore, the reaction between β,γ -alkynyl- α -imino ester **1a** and β -keto ester **2a** using the N,N-dimethylated squaramide (Cat-3') resulted in remarkably lower enantioselectivity (Fig. 5c). This finding underscores the significant importance of potential hydrogen-bonding interactions between the squaramide organocatalyst and substrates. To further clarify the specific interactions between the copper/squaramide catalysis system and the substrates, including ketimino esters and β -keto esters, we performed LC-MS analysis of the reaction solution. We successfully identified the ion peaks of the Cat-3/**1a** complex ([M-Boc]⁺: 801.28; found 801.35) and the Cat-3/Cu/**2b** complex ([M-H]⁺: 832.20; found 831.90) through LC-MS analysis (for details, see the Supplementary Information). A full profile of the model reaction between **1o** and **2b** for the preparation of enantioenriched **4o** was also obtained (Fig. 5d). The ee and dr values of product **4o** was nearly constant during the reaction. Next, we investigated the effect of varying the ratio of Cat-3 to copper salt on the reaction outcome, while maintaining the copper salt loading at 10 mol% (Fig. 5e). It was found that the ee and dr values of the product exhibited significant improvements when the amount of Cat-3 exceeded that of the copper salt. This suggests that the excess portion of Cat-3 may be acting as a ligand for the copper^{65–67}. In addition, reaction progress kinetic analysis using in-situ infrared spectroscopy revealed a second-order dependence on the concentration of Cat-3 (for details, see Supplementary Information, and ReactIR experiments data see Supplementary Dataset 2). Based on the aforementioned mechanistic studies, a tentative Cu/squaramide cooperative catalytic mechanism has been

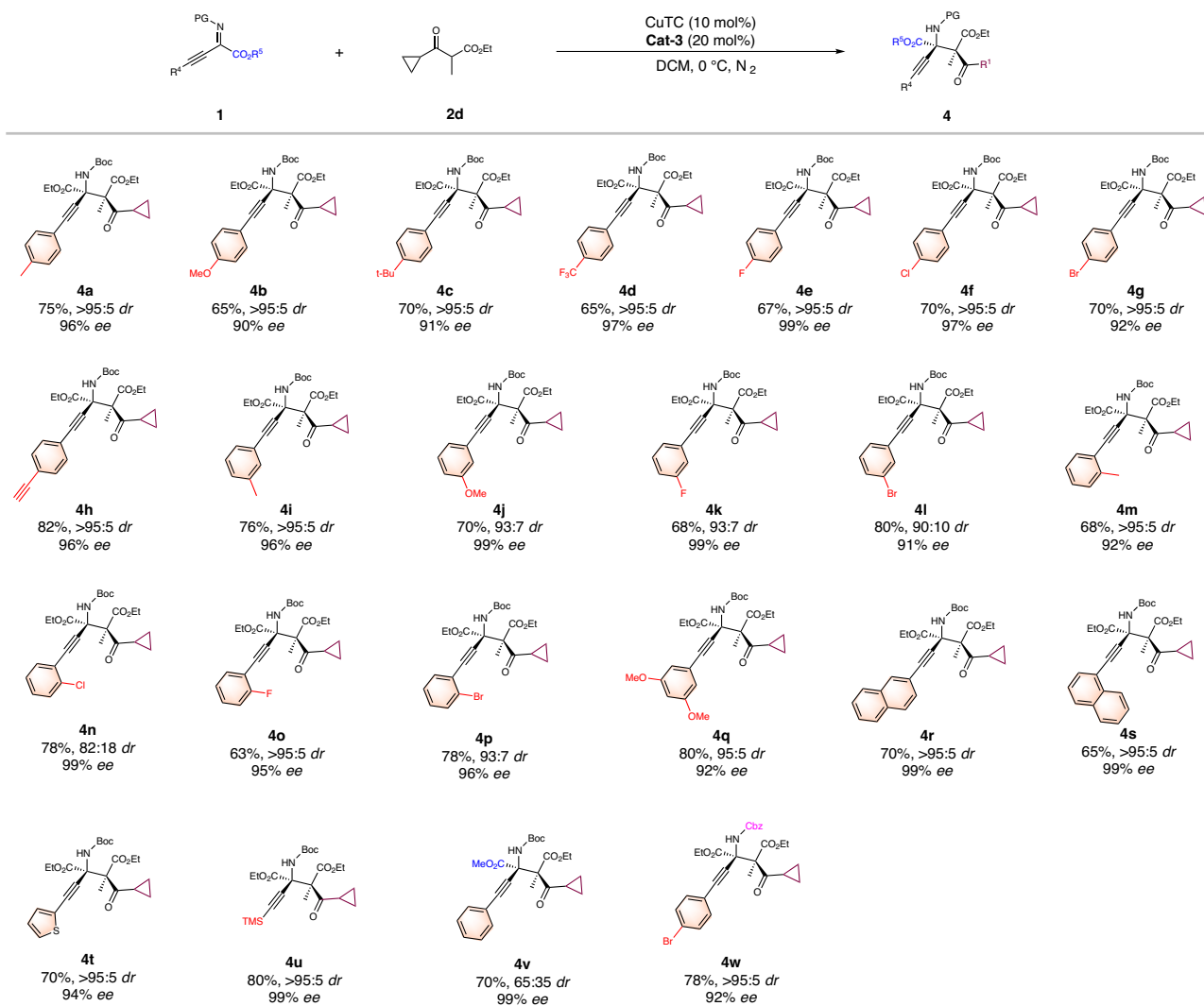
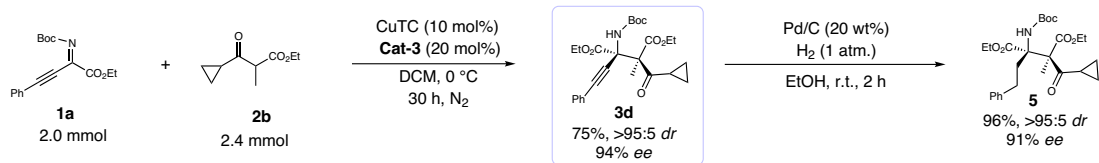


Fig. 3 | Scope of the β,γ -alkynyl- α -imino esters. Conditions: **1** (0.10 mmol), **2** (0.12 mmol), CuTC (10 mol%), Cat-3 (20 mol%), DCM (2.0 mL), at 0 °C for 30–48 h. Boc tert-butoxycarbonyl, TMS trimethylsilyl.

a) The scale-up synthesis and transformation of **3d**



b) The transformation of **3d, **4g** and **4h****

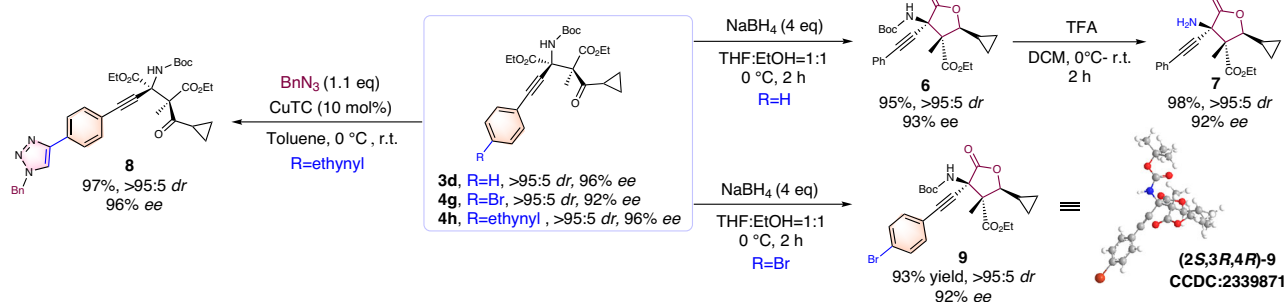


Fig. 4 | Scale-up synthesis and synthetic applications. **a** The scale-up synthesis and transformation of **3d**. **b** The transformation of **3d**, **4g**, and **4h**. Boc tert-butoxycarbonyl, TFA trifluoroacetic acid.

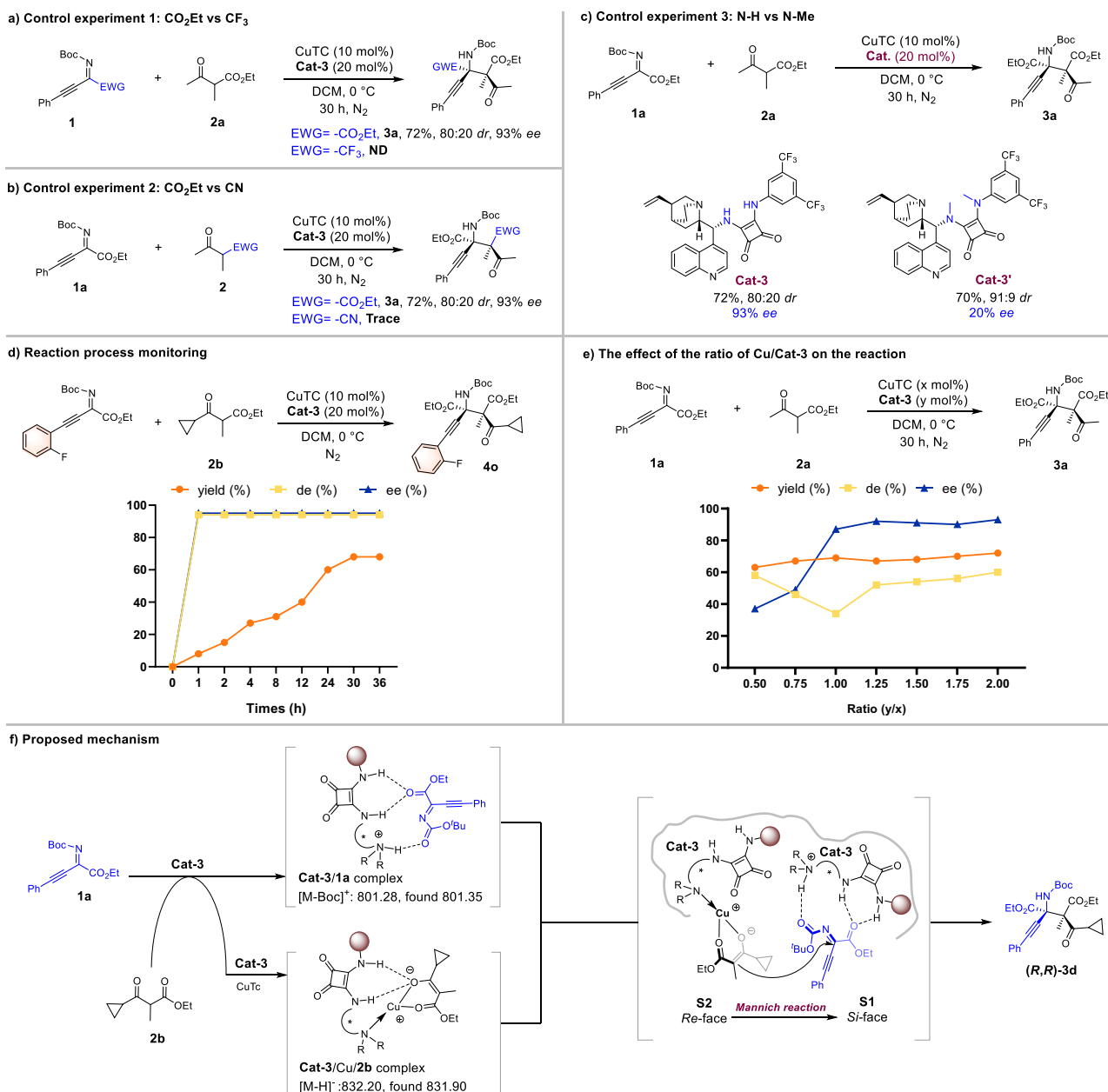


Fig. 5 | Control experiments and mechanistic studies. **a** Control experiment 1: CO₂Et vs CF₃. **b** Control experiment 2: CO₂Et vs CN. **c** Control experiment 3: N-H vs N-Me. **d** Reaction process monitoring. **e** The effect of the ratio of Cu/Cat-3 on the reaction. **f** Proposed mechanism. Boc tert-butoxycarbonyl, ND not detected.

proposed (Fig. 5f). In the presence of a Brønsted base (the tertiary amine moiety of the bifunctional squaramide catalyst) and CuTC, the β -keto ester **2b** undergoes deprotonation and enol tautomerization to form the complex S2 (detected by LC-MS and ¹³C NMR, see the Supplementary Information). Concurrently, another molecule of squaramide catalyst engages in multiple hydrogen-bonding interactions with the N-Boc ketimino ester **1a** to form the intermediate S1. The Cu-bound enolate (complex S2) attacks the hydrogen-bonding activated N-Boc ketimino ester (S1) in an enantio- and diastereoselective manner to give the Mannich product.

DFT calculations. Based on our understanding of the reaction mechanism, the stereo-determining step of this reaction is presumably the nucleophilic addition step forming the C–C bond. DFT calculations were performed to locate transition states for the model reaction between **Cat-3/1a** and the **Cat-3/Cu/2b** complex, elucidating stereoselectivity origins (Fig. 6, see Supplementary Information and Supplementary Dataset 1 for computational details). The results revealed

that **TS-R-R** (0.0 kcal/mol) was the most favorable, stabilized by multiple weak interactions: two hydrogen bonds between the squaramide moiety of **Cat-3** and the methyl ester carbonyl of substrate **1a**, two hydrogen bonds between the amide nitrogen atom of substrate **1a** and the hydrogen atoms on the quinoline ring and adjacent methylene group of **Cat-3**, a stronger O...H–N interaction (1.56 Å) between the protonated bridgehead nitrogen of **Cat-3** and the tert-butyl ester carbonyl of **1a**, and a π – π interaction between the two trifluoromethylphenyl groups of **Cat-3**. These weak interactions stabilized a staggered conformation during C–C bond formation, minimizing steric repulsion. In contrast, **TS-S-S** (2.1 kcal/mol) lacked the variety of weak interactions present in **TS-R-R**, adopting a less favorable configuration with a weaker N...H–N hydrogen bond (1.82 Å), forcing an eclipsed conformation that caused steric clash between the tert-butyl group of **1a** and the ethyl group of **2b** (closest H...H distance 2.03 Å). Diastereomeric transition states were also disfavored: **TS-R-S** (1.8 kcal/mol) featured fewer weak interactions than **TS-R-R** and

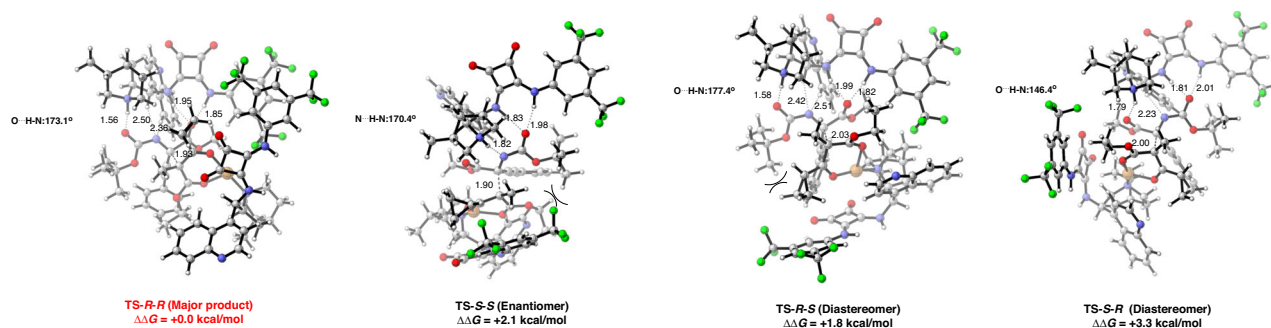


Fig. 6 | DFT-computed transition state structures and relative free energies. Distances between important atoms are in angstrom (Å), bond angles are in degrees.

exhibited steric repulsion (closest H...H distance: 2.29 Å), while **TS-S-R** (3.3 kcal/mol) suffered from a strained O...H-N bond (1.79 Å; angle 146.4°). These energy differences rationalized the high experimental stereoselectivity (96% ee, >95:5 dr), validating the computational stereochemical model.

In summary, drawing inspiration from class II aldolases, we have developed a biomimetic copper-squaramide cooperative catalysis strategy for the asymmetric Mannich reactions, enabling facile access to vicinal tetrasubstituted stereocenters in acyclic systems. Utilizing acyclic ketimines and sterically hindered α -substituted β -keto esters as challenging Mannich substrates, we successfully synthesized highly functionalized amino acid derivatives featuring adjacent and acyclic tetrasubstituted stereocenters with excellent diastereo- and enantioselectivities (up to >19:1 dr and 99% ee). Preliminary mechanistic studies and DFT calculations indicate that the success of this strategy can be attributed to the cooperative roles of the copper salts and the tertiary amine-squaramide organocatalysts, which are crucial for substrate activation and the control of stereoselectivity. Further application of this strategy in other significant asymmetric transformations is underway in our laboratory.

Methods

General information. All reactions were carried out in oven-dried reaction vessel unless otherwise noted and solvents were dried according to established procedures. Reactions were monitored by thin layer chromatography (TLC). Purification of reaction product was carried out by flash chromatography using Qing Dao Sea Chemical Reagent silica gel (200–300 mesh). ^1H , ^{13}C , and ^{19}F NMR spectra were recorded on Bruker 400 MHz or 500 MHz spectrometer in CDCl_3 unless otherwise noted. Chemical shifts in ^1H NMR spectra are reported in parts per million (ppm, δ) downfield from the internal standard Me_4Si (TMS, $\delta = 0$ ppm). Chemical shifts in ^{13}C NMR spectra are reported relative to the central line of the chloroform signal ($\delta = 77.0$ ppm). Data are presented as follows: chemical shift, integration, multiplicity (s = singlet, d = doublet, t = triplet, q = quartet, m = multiplet) and coupling constant in Hertz (Hz). HPLC analyses were conducted on an Agilent instrument using Daicel Chiralpak IA, IB, AD-H, or Chiralcel OD-H columns. High resolution mass spectra were obtained with a Shimadzu LC-MS-IT-TOF mass spectrometer. The single crystal X-ray diffraction studies were carried out on a Xcalibur Onyx Nova diffractometer equipped with $\text{CuK}\alpha$ radiation.

General procedure to prepare chiral products 3 and 4

Conditions: A flame-dried Schlenk tube equipped with a magnetic stirring bar was charged with a mixture of β,γ -alkynyl- α -imino esters **1** (0.10 mmol), a mixture of **CuTC** (10 mol%), **Cat-3** (20 mol%). After being evacuated and backfilled with nitrogen for three times, DCM (1 mL) was added to the Schlenk tube and the mixture was stirred at room temperature under a N_2 atmosphere for 0.5 h. Dicarbonyl compounds **2** (0.12 mmol) in DCM (1 mL) were added sequentially. The

reaction mixture was stirred under a N_2 atmosphere at 0 °C for 30–48 h. When the reaction was complete, the DCM was evaporated in vacuo and the residue was purified by flash silica gel column chromatography (petroleum ether/EtOAc = 5/1) to give products **3** and **4**.

Data availability

The data supporting the findings of this study are available in the manuscript and its Supplementary Information files. Crystallographic data for the structures reported in this Article have been deposited at the Cambridge Crystallographic Data Centre, under deposition numbers CCDC 2339871 (**9**) and CCDC 2452561 (**1p**). Copies of the data can be obtained free of charge via www.ccdc.cam.ac.uk/data_request/cif. All data are available from the corresponding author upon request.

References

- Lovering, F., Bikker, J. & Humblet, C. Es-cape from flatland: increasing saturation as an ap-proach to improving clinical success. *J. Med. Chem.* **52**, 6752–6756 (2009).
- Lovering, F. Escape from flatland 2: complexity and promiscuity. *Med. Chem. Commun.* **4**, 515–519 (2013).
- Ritchie, T. J., Mac-donald, S. J. F., Young, R. J. & Pickett, S. D. The impact of aromatic ring count on compound developa-bility: further insights by examining carbo- and heteroaromatic and -aliphatic ring types. *Drug Discov. Today* **16**, 164–171 (2011).
- Gioranetto, F., Jin, C., Willmore, L., Feher, M. & Shaw, D. E. Fragment hits: what do they look like and how do they bind?. *J. Med. Chem.* **62**, 3381–3394 (2019).
- Geist, E., Kirschning, A. & Schmidt, T. sp^3 - sp^3 Coupling reactions in the synthesis of natural products and biologically active molecules. *Nat. Prod. Rep.* **31**, 441–448 (2014).
- Choi, J. & Fu, G. C. Transition metal-catalyzed alkyl-alkyl bond formation: another dimension in cross-coupling chemistry. *Science* **356**, eaaf7230 (2017).
- Zhao, W.-T. & Shu, W. Enantioselective Csp³-Csp³ formation by nickel-catalyzed enantioconvergent cross-electrophile alkyl-alkyl coupling of unactivated alkyl halides. *Sci. Adv.* **9**, eadg9898 (2023).
- Li, Y. et al. Cobalt-catalysed enantioselective C(sp³)-C(sp³) coupling. *Nat. Catal.* **4**, 901–911 (2021).
- Jing, C., Mao, W. & Bower, J. F. Iridium-catalyzed enantioselective alkene hydroalkylation via a heteroaryl-directed enolization-decarboxylation sequence. *J. Am. Chem. Soc.* **145**, 23918–23924 (2023).
- Peterson, E. A. & Overman, L. E. Contiguous stereogenic quaternary carbons: a daunting challenge in natural products synthesis. *Proc. Natl. Acad. Sci. USA* **101**, 11943–11948 (2004).
- Büschleb, M. et al. Synthetic strategies toward natural products containing contiguous stereogenic quaternary carbon atoms. *Angew. Chem. Int. Ed.* **55**, 4156–4186 (2016).
- Zhou, F. et al. Catalytic enantioselective construction of vicinal quaternary carbon stereocenters. *Chem. Sci.* **11**, 9341–9365 (2020).

13. Long, R., Huang, J., Gong, J. & Yang, Z. Direct construction of vicinal all-carbon quaternary stereocenters in natural product synthesis. *Nat. Prod. Rep.* **32**, 1584–1601 (2015).
14. Feng, J., Holmes, M. & Krische, M. J. Acyclic quaternary carbon stereocenters via enantioselective transition metal catalysis. *Chem. Rev.* **117**, 12564–12580 (2017).
15. Das, J. P. & Marek, I. Enantioselective synthesis of all-carbon stereogenic centers in acyclic systems. *Chem. Commun.* **47**, 4593–4623 (2011).
16. Pierrot, D. & Marek, I. Synthesis of enantioenriched vicinal tertiary and quaternary carbon stereogenic centers within an acyclic chain. *Angew. Chem. Int. Ed.* **59**, 36–49 (2020).
17. Liu, X., Zhao, C., Zhu, R. & Liu, L. Construction of vicinal quaternary carbon stereocenters through diastereo- and enantioselective oxidative 1,6-conjugate addition. *Angew. Chem. Int. Ed.* **60**, 18499–18503 (2021).
18. Næsberg, L. et al. Direct enantio- and diastereoselective oxidative homo-coupling of aldehydes. *Chem. Eur. J.* **24**, 14844–14848 (2018).
19. Huang, X. et al. Palladium-catalysed formation of vicinal all-carbon quaternary centers via propargylation. *Nat. Commun.* **7**, 12382–12390 (2016).
20. Isomura, M., Petrone, D. A. & Carreira, E. M. Construction of vicinal quaternary centers via iridium-catalyzed asymmetric allenyl alkylation of racemic tertiary alcohols. *J. Am. Chem. Soc.* **143**, 3323–3329 (2021).
21. Papidocha, S. M. & Carreira, E. M. Construction of vicinal quaternary centers via Ru-catalyzed enantiospecific allylic substitution with lithium ester enolates. *J. Am. Chem. Soc.* **146**, 23674–23679 (2024).
22. Hethcox, J. C., Shockley, S. E. & Stoltz, B. M. Enantioselective synthesis of vicinal all-carbon quaternary centers via iridium-catalyzed allylic alkylation. *Angew. Chem. Int. Ed.* **57**, 8664–8667 (2018).
23. Zhang, G., Wodrich, M. D. & Cramer, N. Catalytic enantioselective reduction of eschenmoser-slaisen rearrangements. *Science* **383**, 395–401 (2024).
24. Arend, M., Westermann, B. & Risch, N. Modern variants of the Mannich reaction. *Angew. Chem. Int. Ed.* **37**, 1044–1070 (1998).
25. Ting, A. & Schaus, S. E. Organocatalytic asymmetric Mannich reactions: new methodology, catalyst design, and synthetic applications. *Eur. J. Org. Chem.* **35**, 5797–5815 (2007).
26. Arrayás, R. G. & Carretero, J. C. Catalytic asymmetric direct Mannich reaction: a powerful tool for the synthesis of α,β -dimino acids. *Chem. Soc. Rev.* **38**, 1940–1948 (2009).
27. Kobayashi, S., Mori, Y., Fossey, J. S. & Salter, M. M. Catalytic enantioselective formation of C–C bonds by addition to imines and hydrazones: a ten-year update. *Chem. Rev.* **111**, 2626–2704 (2011).
28. Sheng, C., Ling, Z., Luo, Y. & Zhang, W. Cu-catalyzed asymmetric addition of alcohols to β,γ -alkynyl- α -imino esters for the construction of linear chiral N, O-ketals. *Nat. Commun.* **13**, 400–408 (2022).
29. Luo, P. et al. Construction of tetrasubstituted stereocenters via asymmetric catalysis using chiral acyclic secondary amines. *Cell Rep. Phys. Sci.* **3**, 101182 (2022).
30. Verkade, J. M. M., van Hemert, L. J. C., Quaedflieg, P. J. L. M. & Rutjes, F. P. J. T. Organocatalysed asymmetric Mannich reactions. *Chem. Soc. Rev.* **37**, 29–41 (2008).
31. Shibasaki, M. & Yoshikawa, N. Lanthanide complexes in multifunctional asymmetric catalysis. *Chem. Rev.* **102**, 2187–2210 (2002).
32. Friestad, G. K. & Mathies, A. K. Recent developments in asymmetric catalytic addition to C=N bonds. *Tetrahedron* **63**, 2541–2569 (2007).
33. Shibasaki, M., Kanai, M., Matsu-naga, S. & Kumagai, N. Recent progress in asymmetric bifunctional catalysis using multimetallic systems. *Acc. Chem. Res.* **42**, 1117–1127 (2009).
34. Trost, B. M. & Bartlett, M. J. ProPhenol-catalyzed asymmetric additions by spontaneously assembled dinuclear main group metal complexes. *Acc. Chem. Res.* **48**, 688–701 (2015).
35. Liu, S., Gao, J., Zou, Y. & Hai, Y. Enzymatic synthesis of unprotected α,β -diamino acids via direct asymmetric Mannich reactions. *J. Am. Chem. Soc.* **146**, 20263–20269 (2024).
36. Zhu, L. & Wang, D. Deciphering the cooperative effect of base and N-substituents on the origin of enantioselectivity switching for Mannich reactions of glycinate by carbonyl catalysts. *J. Catal.* **415**, 1–11 (2022).
37. Yamashita, Y., Noguchi, A., Fushimi, S., Hatanaka, M. & Kobayashi, S. Chiral metal salts as ligands for catalytic asymmetric Mannich reactions with simple amides. *J. Am. Chem. Soc.* **143**, 5598–5604 (2021).
38. Chen, J. et al. Carbonyl catalysis enables a biomimetic asymmetric Mannich reaction. *Science* **360**, 1438–1442 (2018).
39. Wang, Y. et al. Asymmetric synthesis of synpropargylamines and unsaturated β -amino acids under Brønsted base catalysis. *Nat. Commun.* **6**, 8544–8552 (2015).
40. Dai, J. et al. Enantiodivergence by minimal modification of an acyclic chiral secondary aminocatalyst. *Nat. Commun.* **10**, 5182–5189 (2019).
41. You, Y., Zhang, L., Cui, L., Mi, X. & Luo, S. Catalytic asymmetric Mannich reaction with N-carbamoyl imine surrogates of formaldehyde and glyoxylate. *Angew. Chem. Int. Ed.* **56**, 13814–13818 (2017).
42. Trost, B. M., Tracy, J. S., Yusoon, T. & Hung, C. I. J. Acyclic branched α -fluoro ketones for the direct asymmetric Mannich reaction leading to the synthesis of β -tetrasubstituted β -fluoro amines. *Angew. Chem. Int. Ed.* **59**, 2370–2374 (2020).
43. Homma, C., Takeshima, A., Kano, T. & Maruoka, K. Construction of chiral α -tert-amine scaffolds via amine-catalyzed asymmetric Mannich reactions of alkyl-substituted ketimines. *Chem. Sci.* **12**, 1445–1450 (2021).
44. Li, G. et al. Water enables diastereodivergency in bispidine-based chiral amine-catalyzed asymmetric Mannich reaction of cyclic N-sulfonyl ketimines with ketones. *Chem. Sci.* **13**, 4313–4320 (2022).
45. Engl, O. D., Fritz, S. P. & Wennemers, H. Stereoselective organocatalytic synthesis of oxindoles with adjacent tetrasubstituted stereocenters. *Angew. Chem. Int. Ed.* **54**, 8193–8197 (2015).
46. Takeda, T., Kondoh, A. & Terada, M. Construction of vicinal quaternary stereogenic centers by enantioselective direct Mannich-type reaction using a chiral bis(guanidino)iminophosphorane catalyst. *Angew. Chem. Int. Ed.* **55**, 4734–4737 (2016).
47. Ding, R., De los Santos, Z. A. & Wolf, C. Catalytic asymmetric Mannich reaction of α -fluoronitriles with ketimines: enantioselective and diastereodivergent construction of vicinal tetrasubstituted stereocenters. *ACS Catal.* **9**, 2169–2176 (2019).
48. Trost, B. M., Hung, C. I. & Scharf, M. J. Direct catalytic asymmetric vinylogous additions of α,β - and β,γ -butenolides to polyfluorinated alkynyl ketimines. *Angew. Chem. Int. Ed.* **57**, 11408–11412 (2018).
49. Zhang, H.-J., Xie, Y.-C. & Yin, L. Copper(I)-catalyzed asymmetric decarboxylative Mannich reaction enabled by acidic activation of 2H-azirines. *Nat. Commun.* **10**, 1699–1707 (2019).
50. Xu, J. et al. Sterically hindered and deconjugative α -regioselective asymmetric Mannich reaction of Meinwald rearrangement intermediate. *Angew. Chem. Int. Ed.* **62**, e202217887 (2023).
51. Zhu, W.-R. et al. Catalytic asymmetric synthesis of vicinal tetrasubstituted diamines via umpolung cross-Mannich reaction of cyclic ketimines. *Org. Lett.* **22**, 5014–5019 (2020).
52. Xiao, X. et al. Biomimetic asymmetric catalysis. *Sci. China Chem.* **66**, 1553–1633 (2023).

53. Lovinger, G. J., Sak, M. H. & Jacobsen, E. N. Catalysis of an S_N2 pathway by geometric preorganization. *Nature* **632**, 1052–1059 (2024).
54. Machajewski, T. D. & Wong, C.-H. The catalytic asymmetric Aldol reaction. *Angew. Chem. Int. Ed.* **39**, 1352–1375 (2000).
55. Takemoto, Y. Recognition and activation by ureas and thioureas: stereoselective reactions using ureas and thioureas as hydrogen-bonding donors. *Org. Biomol. Chem.* **3**, 4299–4306 (2005).
56. Malerich, J. P., Hagihara, K. & Rawal, V. H. Chiral squaramide derivatives are excellent hydrogen bond donor catalysts. *J. Am. Chem. Soc.* **130**, 14416–14417 (2008).
57. Alemán, J., Parra, A., Jiang, H. & Jørgensen, K. A. Squaramides: bridging from molecular recognition to bifunctional organocatalysis. *Chem. -Eur. J.* **17**, 6890–6899 (2011).
58. Gong, L.-Z. *Asymmetric Organo-Metal Catalysis: Concepts, Principles, and Applications*. (Wiley-VCH: Weinheim, Germany, 2021).
59. Gong, L.-Z. Asymmetric organocatalysis combined with metal catalysis: a promising and emerging field. *Acta Chim. Sin.* **76**, 817–818 (2018).
60. Xiao, X., Lin, L., Lian, X., Liu, X. & Feng, X. Catalytic asymmetric α -amination of β -keto esters and β -keto amides with a chiral N, N'-dioxide-copper(I) complex. *Org. Chem. Front.* **3**, 809–812 (2016).
61. Wu, H., Andres, R., Wang, Q. & Zhu, J. Catalytic enantioselective α -ketol rearrangement. *Angew. Chem. Int. Ed.* **58**, 499–503 (2019).
62. Davies, I. W., Gerena, L., Lu, N., Larsen, R. D. & Reider, P. J. Concise synthesis of conformationally constrained pybox ligands. *J. Org. Chem.* **61**, 9629–9630 (1996).
63. Müller, D., Umbricht, G. & Weber, B. & Pfaltz, a. C_2 -Symmetric 4,4',5,5'-tetrahydrobi(oxazoles) and 4,4',5,5'-tetrahydro-2,2'-methylenebis[oxazoles] as chiral ligands for enantioselective catalysis preliminary communication. *Helv. Chim. Acta* **74**, 232–240 (1991).
64. Johnson, J. S. & Evans, D. A. Chiral bis(oxazoline) copper(II) complexes: versatile catalysts for enantioselective cycloaddition, Aldol, Michael, and carbonyl ene reactions. *Acc. Chem. Res.* **33**, 325–335 (2000).
65. Li, M. et al. Highly enantioselective carbene insertion into N–H bonds of aliphatic amines. *Science* **366**, 990–994 (2019).
66. Furniel, L. G., Echemendía, R. & Burtoloso, A. C. B. Cooperative copper-squaramide catalysis for the enantioselective N–H insertion reaction with sulfoxonium ylides. *Chem. Sci.* **12**, 7453–7459 (2021).
67. Gu, X. et al. Catalytic asymmetric P–H insertion reactions. *J. Am. Chem. Soc.* **145**, 20031–20040 (2023).

Acknowledgements

This work was financially supported by Guangdong Basic and Applied Basic Research Foundation (No. 2024A1515010680, J.W.), Guangxi Natural Science Foundation (No. 2021GXNSFDA075016, J.W.), Guangxi Key R&D Program Project (No. AB25069063, W.-R.Z.), Guangdong Provincial Key Laboratory of Chiral Molecule and Drug Discovery (No. 2019B030301005, J.W.), Guangdong Provincial Key Laboratory of Construction Foundation (No. 2023B1212060022, J.W.), Guangzhou Science and Technology Programme-2024 Basic and Applied Basic

Research Theme-Young Doctoral 'Sailing' Project (No. SL2023A04J02304, W.-R.Z.), Guangdong Pharmaceutical University's "Discipline Training Excellence, Innovation and Quality Improvement" Engineering Team Project (No. 2024QZ03 and 2024ZZ05, W.-R.Z.), Administration of Traditional Chinese Medicine of Guangdong Province, China (No. 20241164, W.-R.Z.).

Author contributions

W.-R.Z., Z.-L.O. and Y.-Z.L. performed the experiments and wrote the draft. P.Y. and X.D. performed the DFT calculation and wrote the draft. X.-Y. D., Y.-J. X. and J.-X.Z. carried out experiments and prepared the Supplementary Information. P.Y., G.L., A.S.C.C. and J.W. analyzed the results. G.L. and J.W. conceived and directed the project and wrote the paper.

Competing interests

The authors declare no competing interests.

Additional information

Supplementary information The online version contains supplementary material available at <https://doi.org/10.1038/s41467-025-63919-9>.

Correspondence and requests for materials should be addressed to Peiyuan Yu, Gui Lu or Jiang Weng.

Peer review information *Nature Communications* thanks Jie Han and the other anonymous reviewer(s) for their contribution to the peer review of this work. A peer review file is available.

Reprints and permissions information is available at <http://www.nature.com/reprints>

Publisher's note Springer Nature remains neutral with regard to jurisdictional claims in published maps and institutional affiliations.

Open Access This article is licensed under a Creative Commons Attribution-NonCommercial-NoDerivatives 4.0 International License, which permits any non-commercial use, sharing, distribution and reproduction in any medium or format, as long as you give appropriate credit to the original author(s) and the source, provide a link to the Creative Commons licence, and indicate if you modified the licensed material. You do not have permission under this licence to share adapted material derived from this article or parts of it. The images or other third party material in this article are included in the article's Creative Commons licence, unless indicated otherwise in a credit line to the material. If material is not included in the article's Creative Commons licence and your intended use is not permitted by statutory regulation or exceeds the permitted use, you will need to obtain permission directly from the copyright holder. To view a copy of this licence, visit <http://creativecommons.org/licenses/by-nc-nd/4.0/>.

© The Author(s) 2025